

Mathematical modeling of a DC motor with separate excitation

Modelo matemático de un motor de corriente continua con excitación separada

Carlos A. Reyes G.

Universidad Distrital Francisco José de Caldas
carareyesg@correo.udistrital.edu.co

Gustavo S. Gerena T.

Universidad Distrital Francisco José de Caldas
gsgerenat@correo.udistrital.edu.co

This article proposes a model for a direct current motor with separate excitation using speed control by armature current. Based on an understanding of its electromechanical functioning and an adequate conceptualization of both the laws of physics and mathematical structure, this model is constructed as a fundamental exercise for the development of control and simulation schemes. To evaluate the performance of the model, performance curves are presented for a test machine.

Keywords: Control, DC motor, dynamic systems, electromagnetism, electromechanical, modeling, separate excitation

Este artículo propone un modelo para un motor de corriente continua con excitación separada que utiliza control de velocidad por corriente de armadura. A partir de la comprensión de su funcionamiento electromecánico y una adecuada conceptualización tanto de leyes de la física como de la estructura matemática, se construye dicho modelo como ejercicio fundamental para el desarrollo de esquemas de control y simulación. Para evaluación del desempeño del modelo se presentan curvas de comportamiento para una máquina de prueba.

Palabras clave: Control, electromagnetismo, electromecánico, excitación separada, modelado, motor CC, sistemas dinámicos

Article typology: Research

Date manuscript received: December 6, 2017

Date manuscript acceptance: December 15, 2017

Research funded by: Universidad Distrital Francisco José de Caldas.

How to cite: Reyes, C., Gerena, G. (2018). *Mathematical modeling of a DC motor with separate excitation.* Tekhnê, 15(1), 13 -20.

Introduction

The DC motor is, in short, a torque transducer that transforms electrical energy into mechanical energy (Kuo, 2002). It is an important source of driving energy in today's industrial and technological world, and it also outperforms alternating current motors due to its high controllability of speed and torque (Gordillo & Martínez, 2018).

The superior performance of the DC motor means that it makes it possible to more easily perform some functions that the AC motor does not achieve (Martínez & Galvis, 2006). Two examples of this are the DC motor's ability to develop torque several times greater in magnitude than an AC motor of a similar size and the ability to operate at speeds unreachable by an AC motor.

This document proposes an approximate mathematical model of the DC motor for this purpose of great utility in both education and research (Martínez, Montiel, & Jacinto, 2016). We construct an equivalent circuit of the device, and then we define the set of mathematical expressions that allow linking the physical variables that constitute the proposed model. The constant values of the model were taken from articles with models evaluated for the same type of electric machine in order to compare the result obtained (Alvarez, 2012).

Once the differential expression that relates the variables of interest has been developed, they are taken to the frequency domain through the application of the Laplace transform. Then the expression for the angular velocity ω is solved, the constants are replaced by the reference values, and finally, the inverse Laplace transform is applied to return to the time domain.

The resulting expression will then be the solution of the proposed model, and will, therefore, describe the behavior of the angular velocity of the motor as a function of time.

In the second part of the article, graphical information on the behavior of angular velocity as a function of time is obtained using the SIMULINK simulator, which offers a graphical user interface (GUI) useful enough to build models and to examine how successful the model developed has been. The final part of the article shares the results and builds conclusions.

Background and current status of the DC motor

The Nikola Tesla Alternating Current (AC) induction motor can be considered as the cornerstone of the triumph of alternating current over the direct current system (Brittain, 2005). However, there is one aspect where the contest does not seem to have shifted to alternating current, and that is what has allowed direct current motors to be so important today. Observability and controllability are two essential factors in the analysis of dynamic systems, the latter being the most important advantage of the DC motor over the AC

motor, as it allows a greater range and degree of control over speed and torque.

In fact, the development of DC motors continues to advance, as evidenced, for example, by the work of electrical engineer and renowned inventor Frank Julian Sprague, who was recently honored in The History column in the November-December 2015 issue of IEEE Power & Energy journal (Sprague, 2015). Sprague's work pioneered the invention and development of constant speed DC motors, which, in addition to being non-slip, are completely self-regulating, even under variable loads (Kuo, 2002). This certainly expands the frontier of possibilities for the DC motor, and also justifies the objective of this paper.

One of the critical points of the DC motor has been the brushes collector system since the wear of the brushes due to friction, maintenance and the associated cost have reduced the efficiency of the machine. Currently, however, not only are new prototypes of brushless DC motors (BLDC motors) being worked on, but the effectiveness of automatic adjustment with PID controllers (Pongfai & Assawinchaichote, 2017) has even been increased by applying artificial intelligence (AI) algorithms (García, Osuna, & Martínez, 2018; Montiel, Martínez, & Jacinto, 2017).

Description and principle of operation of the DC motor

In the following, we present a schematic description of the engine and a synthesis of its basic operating principle.

As can be seen in Fig. 1, the direct current motor is a machine composed of two parts, rotor **A** which is a sweet steel cylinder mounted on a shaft that can rotate on its axis, and stator or casing **M** where the permanent magnets or electromagnets are located if there are field coils **F** and **F'**. In any case, the stator or inductor guarantees a magnetic field between **P** and **P'** as indicated by the dotted lines.

It should be pointed out that these field lines describe the trajectories indicated as long as the rotor turns counterclockwise as a result of the interaction between the magnetic field of the inductor and the electric field of the armature. This dynamic happens because a current enters through the brushes or carbons on the brush collector and circulates through the **C** conductors.

Fig. 2 shows the front and side views of rotor **A** in Fig. 1. Note that Fig. 1 does not show either the brush collector or the brushes for simplicity. The magnetic flux ϕ comes from the stator.

The first step in modeling a system, in this case, the DC motor, is to understand its operating principle, so below we make a brief description of it.

By means of an excitation source v_a , an electric charge is circulated through the conductor of the armature, generating an i_a current. This current gives rise to an electric field that gives rise to a magnetic field, this phenomenon is

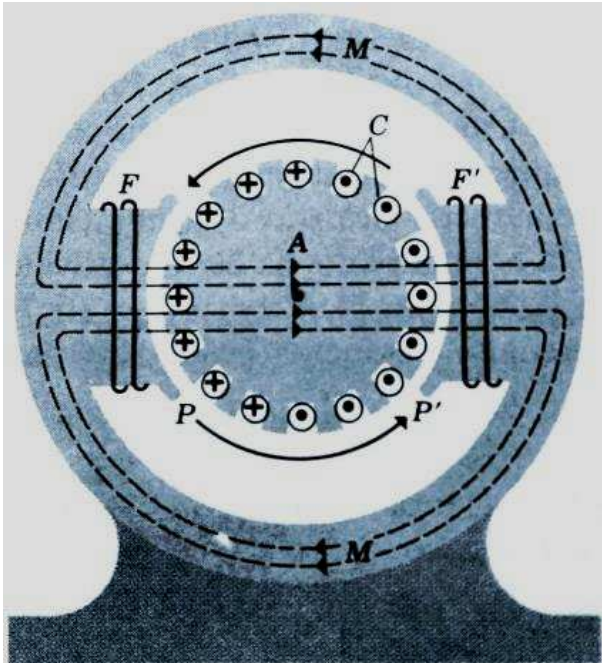


Figure 1. Schematic diagram of the operation of a DC motor (Kuo, 2002).

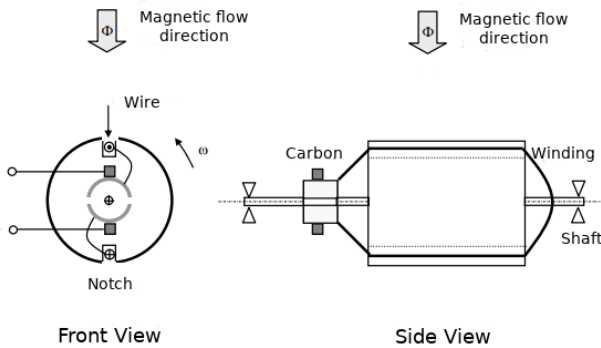


Figure 2. Schematic diagram of a DC motor.

described by Maxwell's equations (Kuo, 2002). When the rotor field interacts with the magnetic field provided by the permanent magnet, the rotation of the armature is generated, a movement called torque. This phenomenon is described by the Lorentz force equation which says that a conductor carrying current experiences a force that tends to move it when placed in a magnetic field (Kuo, 2002) and by Lenz's Law which states that the direction of an induced current is such that it opposes the cause that produces it (Kuo, 2002). It is interesting that according to the above it is possible to infer that the DC motor operates under electromechanical principles and that the torque that is a mechanical variable can be controlled from electrical variables.

Once the principle of operation is understood the next step is to elaborate the approximate equivalent circuit taking into account that:

- The armature winding can be modeled as a series RL circuit.
- In the rotor, a fem or force counter electromotive v_b is induced according to the Faraday induction law (Kuo, 2002).
- A direct voltage source v_a is applied to the armature terminals.

The Kirchhoff tension law can then be applied to construct the first expression that relates the variables v_a , R_a , L_a , and v_b , to the equivalent circuit shown in Fig. 3.

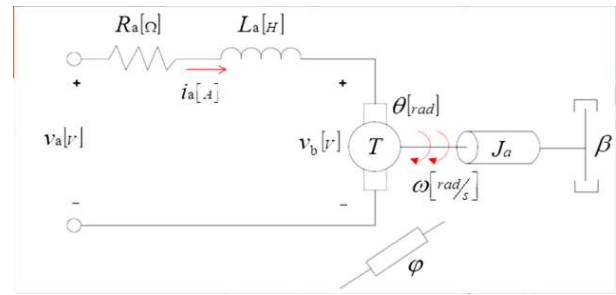


Figure 3. Equivalent circuit of the motor system in direct current, separately excited.

Where:

- R_a represents the natural resistance of the conductor forming the armature winding in ohms.
- L_a is the value of the armature winding inductance in henrys.
- v_a is the DC voltage applied to the armature circuit in volts.
- i_a denotes the current flowing through the armature conductor in amperes.
- v_b represents the counter-electromotive force in volts.
- ϕ represents the stator's fixed magnetic field.
- θ represents the angular displacement of the rotor in radians.
- ω is the rotor angular velocity in rad/s.
- J_a denotes the equivalent rotational inertia of the rotor shaft in kilograms.
- β is the coefficient of viscous friction in N·m·s.
- τ_f is the friction force or viscous damping in Newtons.
- τ_e is the electromagnetic torque in Newtons.
- τ_c is the resulting torque in Newtons.
- k_p is the electromagnetic torque constant in N·m/A.
- k_b is the counter electromotive force constant.

Analysis for choice of variables and construction of the mathematical model

Making use of Kirchhoff's voltage law in the equivalent circuit shown in Fig. 3 relating to v_a , R_a , L_a and v_b can be obtained:

$$v_a(t) = v_{Ra}(t) + v_{La}(t) + v_b(t) \quad (1)$$

Expressing Eq. 1 in terms of the current:

$$v_a(t) = R_a i_a(t) + L_a \frac{di_a(t)}{dt} + v_b(t) \quad (2)$$

The value of the counter electromotive force v_b is defined as shown in Eq. 3. Replacing this expression in Eq. 2 results in Eq. 4:

$$v_b(t) = k_b \omega(t) \quad (3)$$

$$v_a(t) = R_a i_a(t) + L_a \frac{di_a(t)}{dt} + k_b \omega(t) \quad (4)$$

Then Eq. 4 is the first differential equation of the model and describes the electrical part of the system.

For the description of the mechanical part, it is necessary to find the second differential expression. As it is a linear system, it is assumed that the torque developed by the motor is proportional to the flow between the iron and the armature current. In other words, it is possible to conceptualize an equation of torques that relates the applied force or resultant torque τ_c , the inertia of the armature τ_e and the friction force τ_f which, said to be a step, depends on the angular velocity ω , and opposes the movement. So:

$$\tau_c(t) = \tau_e(t) - \tau_f(t) \quad (5)$$

In addition τ_c is described by the expression:

$$\tau_c(t) = J_a \cdot \frac{d\omega(t)}{dt} \quad (6)$$

The resulting torque τ_c is generated by the electromagnetic torque τ_e , which in turn depends on the armature current i_a and is defined as:

$$\tau_e(t) = k_p \cdot i_a(t) \quad (7)$$

Where k_p is the electromagnetic torque constant. The viscous damping τ_f , or viscous friction force, is defined as:

$$\tau_f(t) = \beta \cdot \omega(t) \quad (8)$$

Now, replacing Eqs. 6, 7 and 8 in Eq. 5 gives:

$$J_a \cdot \frac{d\omega(t)}{dt} = k_p \cdot i_a(t) - \beta \cdot \omega(t) \quad (9)$$

Solving for $i_a(t)$ in Eq. 9, results:

$$i_a(t) = \frac{J_a \cdot \frac{d\omega(t)}{dt} + \beta \cdot \omega(t)}{k_p} \quad (10)$$

Then, deriving the Eq. 10 is obtained:

$$\frac{di_a(t)}{dt} = \frac{J_a \cdot \frac{d^2\omega(t)}{dt^2} + \beta \cdot \frac{d\omega(t)}{dt}}{k_p} \quad (11)$$

Which is the second differential equation of the system, and describes the mechanical part of it. Finally, to obtain the differential equation that integrates the electrical and mechanical parts, Eqs. 10 and 11 are substituted in Eq. 4, from where it results:

$$v_a(t) = R_a \left[\frac{J_a \frac{d\omega(t)}{dt} + \beta \cdot \omega(t)}{k_p} \right] + L_a \left[\frac{J_a \frac{d^2\omega(t)}{dt^2} + \beta \cdot \frac{d\omega(t)}{dt}}{k_p} \right] + k_b \omega(t) \quad (12)$$

It is important to note that this expression relates to electrical variables such as current and voltage with mechanical variables such as torque and friction force, which is consistent because it is an electromechanical system in itself.

Eq. 12 describes the mathematical model of the separately excited DC motor. Before proceeding with the solution of the mathematical model it must be considered that Eq. 12 is a second order differential equation, but it must also be taken into account that the value of L approaches zero in direct current motors with independent excitation, so Eq. 12 can be simplified to a first-order homogeneous, linear differential equation of constant coefficients.

$$v_a(t) = R_a \left[\frac{J_a \frac{d\omega(t)}{dt} + \beta \cdot \omega(t)}{k_p} \right] + k_b \cdot \omega(t) \quad (13)$$

Mathematical model solution

In order to be able to apply the transform of Laplace, it is necessary to establish that $\omega(0) = 0$. Then Eq. 13 is transformed as follows:

$$\mathcal{L}[v_a(t)] = \frac{J_a R_a}{k_p} \cdot \mathcal{L}\left[\frac{d\omega(t)}{dt}\right] + R_a \cdot \mathcal{L}\left[\frac{\beta \cdot \omega(t)}{k_p}\right] + \mathcal{L}[k_b \cdot \omega(t)] \quad (14)$$

$$\frac{V_a(s)}{s} = \frac{J_a \cdot R_a}{k_p} \cdot s \cdot W(s) + \frac{R_a \cdot \beta}{k_p} W(s) + k_b \cdot W(s) \quad (15)$$

Factoring $W(s)$:

$$\frac{V_a(s)}{s} = W(s) \cdot \left[\frac{J_a \cdot R_a}{k_p} \cdot s + \frac{R_a \cdot \beta}{k_p} + k_b \right] \quad (16)$$

By doing:

$$\frac{J_a \cdot R_a}{k_p} = \lambda \quad \text{and} \quad \frac{R_a \cdot \beta}{k_p} + k_b = \delta \quad (17)$$

And rewriting Eq. 16 comes out:

$$\frac{V_a(s)}{s} = W(s) \cdot (\lambda s + \delta) \quad (18)$$

Solving for $W(s)$:

$$W(s) = \frac{V_a(s)}{s(\lambda s + \delta)} \quad (19)$$

The partial fraction method is now applied to Eq. 19.

$$W(s) = V_a(s) \cdot \left[\frac{A}{s} + \frac{B}{(\lambda s + \delta)} \right] \quad (20)$$

$$V_a(s) \cdot \left[\frac{1}{s(\lambda s + \delta)} \right] = V_a(s) \cdot \left[\frac{A}{s} + \frac{B}{(\lambda s + \delta)} \right] \quad (21)$$

$$\left(\frac{1}{s(\lambda s + \delta)} \right) = \left(\frac{A}{s} + \frac{B}{(\lambda s + \delta)} \right) \quad (22)$$

$$1 = A(\lambda s + \delta) + B \cdot s \quad (23)$$

$$1 = A\lambda s + A\delta + B \cdot s \quad (24)$$

$$s \cdot (0) + 1 = s(A\lambda + B) + A\delta \quad (25)$$

Then we get that:

$$1 = A\delta \implies A = \frac{1}{\delta} \quad (26)$$

$$0 = A\lambda + B \implies B = -A\lambda \implies B = -\frac{\lambda}{\delta} \quad (27)$$

And Eq. 20 becomes:

$$W(s) = V_a(s) \cdot \left[\frac{\frac{1}{\delta}}{s} + \frac{-\frac{\lambda}{\delta}}{(\lambda s + \delta)} \right] \quad (28)$$

Dividing between λ numerator and denominator of the second term of the bracket, and factoring $1/\delta$ to bring the expression to a known form we obtain:

$$W(s) = \frac{V_a(s)}{\delta} \cdot \left[\frac{1}{s} - \frac{1}{\left(s + \frac{\delta}{\lambda}\right)} \right] \quad (29)$$

Now Laplace inverse transform is applied to return to the time domain and obtain the Eq. 31 which is the solution of the model in the time domain.

$$\mathcal{L}^{-1}[W(s)] = \frac{v_a(t)}{\delta} \cdot \mathcal{L}^{-1}\left[\frac{1}{s}\right] - \frac{v_a(t)}{\delta} \cdot \mathcal{L}^{-1}\left[\frac{1}{\left(s + \frac{\delta}{\lambda}\right)}\right] \quad (30)$$

$$\omega(t) = \frac{v_a(t)}{\delta} \left[1 - e^{-\frac{\delta}{\lambda}t} \right] \quad (31)$$

Table 1

Experimental data of the DC motor:

Armature and load data			
Magnitude	Symbol	Value	Unit
Excitation voltage	v_a	240	V
Electric current	i_a	16.2	A
Resistance	R_a	0.6	Ω
Inductance	L_a	0.0012	H
Counter-electromotive force constant	k_b	1.8	V s
Electromagnetic torque constant	k_p	0.4	N m/A
Rotor rotational inertia	J_a	1	kg/m ²
Coefficient of viscous friction	β	0.2287	N m s

Finally, we return the replacement of δ and λ and replace the values of J_a , R_a , k_b , β , and k_p supplied by the reference article (table 1).

$$\omega(t) = \frac{v_a(t)}{\frac{R_a\beta}{k_p} + k_b} \left[1 - e^{-\frac{\frac{R_a\beta}{k_p} + k_b}{J_a R_a} t} \right] \quad (32)$$

Finally Eq. 33 is obtained, after replacing the parametric values given in the reference article.

$$\omega(t) = 111.99 \cdot \left[1 - e^{-1.4287t} \right] \quad (33)$$

Simulations

Below are graphs of torque, angular velocity, armature current, and counter-electromotive force obtained with the Simulink simulator. The construction was done using block diagrams (Figs. 4, 5 and 6, Fig. 4 shows the block diagram used in the simulation, Fig. 5 shows the block diagram for angular velocity, and Fig. 6 shows the block diagram for armature current) from the differential relationships obtained by solving $di(t)/dt$ in Eq. 4 and $d\omega(t)/dt$ in Eq. 9.

Fig. 7 shows the behaviour of the angular velocity as a function of time.

Fig. 8 shows the behavior of the armature current as a function of time.

Fig. 9 shows the torque as a function of time.

Fig. 10 shows the counter-electromotive force as a function of time.

Conclusions

The mathematical model of the DC motor with independent excitation can be described by the expression:

$$\omega(t) = \frac{v_a(t)}{\frac{R_a\beta}{k_p} + k_b} \left[1 - e^{-\frac{\frac{R_a\beta}{k_p} + k_b}{J_a R_a} t} \right] \quad (34)$$

This equation can be easily implemented in simulation software such as Simulink for specific values of machine

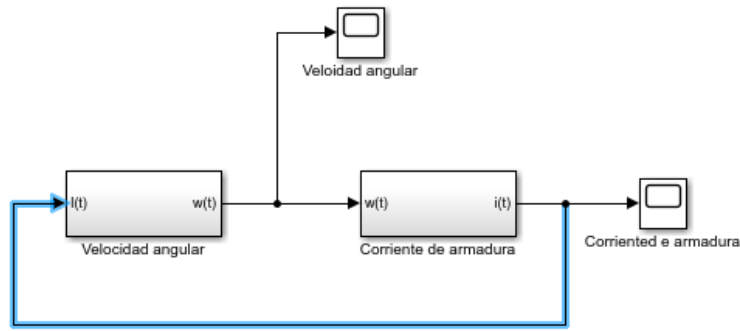


Figure 4. Diagram of blocks and subsystems used in the simulation.

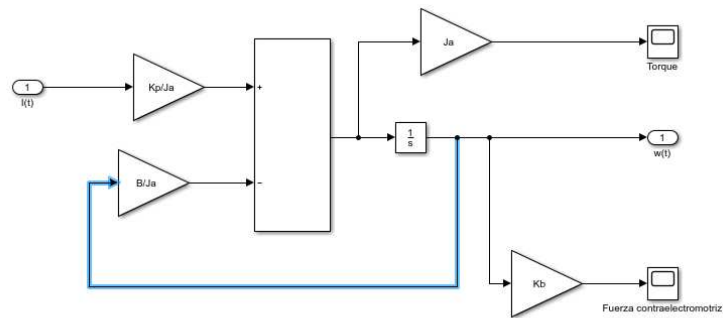


Figure 5. Angular velocity subsystem diagram.

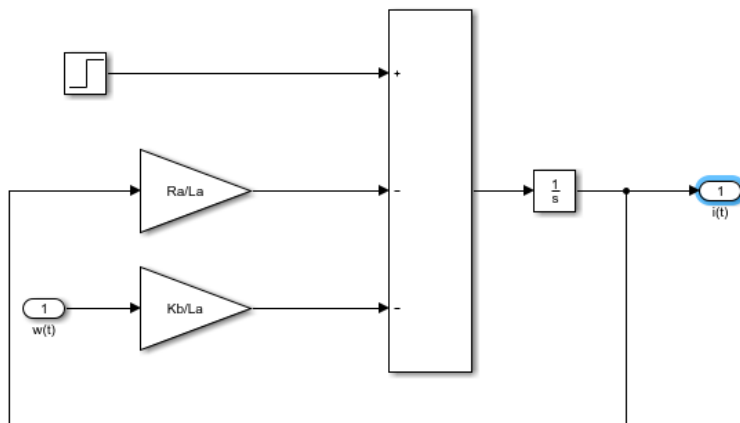


Figure 6. Block diagram for armature current.

parameters, and derive with respect to time the behavior of both the angular velocity and the armature current and torque developed. It is even possible to consider more complex situations, for example, to vary the value of the armature resistance over time as if it were a variable resistance in the machine, or to vary the armature voltage to analyze the behavior of a speed control scheme. The test curves developed for the machine matched those reported in articles

for the same machine parameters, validating the behavior of the model.

References

- Alvarez, M. (2012). Modelo matemático de un motor de corriente continua separadamente excitado: Control de velocidad por corriente de armadura. *Latin-American Journal of Physics Education*, 6(1), 155-161.

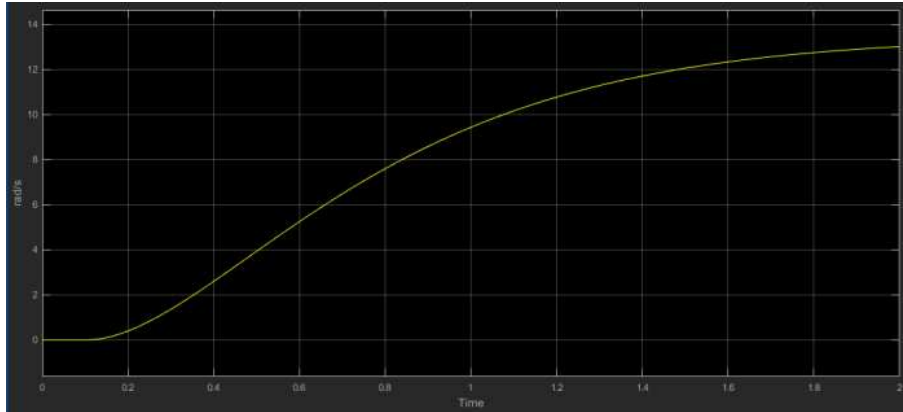


Figure 7. Angular speed.

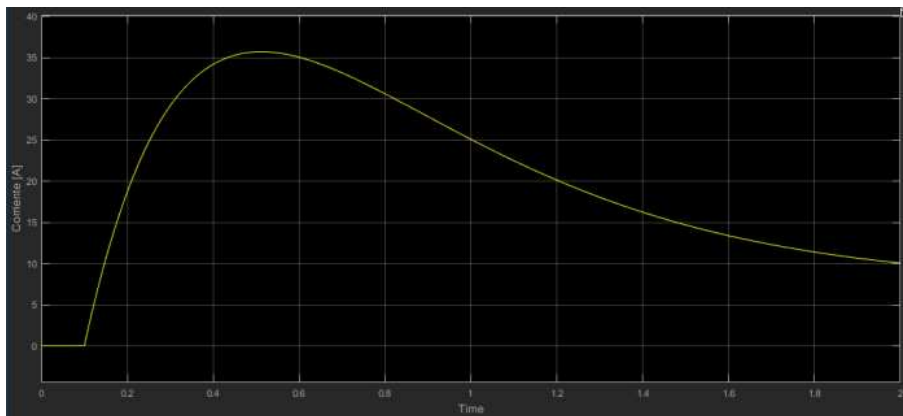


Figure 8. Armature current.

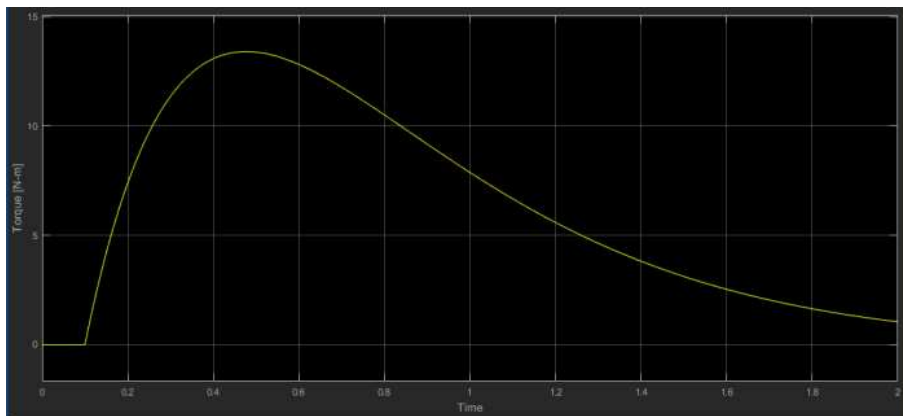


Figure 9. Torque as a function of time.

Brittain, J. (2005). Electrical engineering hall of fame: Nikola tesla. *Proceedings of the IEEE*, 93(5), 1057-1059.

García, C., Osuna, B., & Martínez, F. (2018). Safe grasping system for robotic hand with fingers. *Contemporary Engineering Sciences*, 11(40), 1991-1998.

Gordillo, J., & Martínez, F. (2018). Fuzzy control for bipedal robot considering energy balance. *Contemporary*

Engineering Sciences, 11(39), 1945-1952.

Kuo, B. (2002). *Automatic control systems* (Vol. 8). Wiley.

Martínez, F., & Galvis, J. (2006). Control escalar en motores de inducción monofásicos. *Tecnura*, 10(19), 29-37.

Martínez, F., Montiel, H., & Jacinto, E. (2016). Inductive teaching and problem-based learning as significant training tools in electrical engineering. *Smart Innovation, Systems and Technologies*, 59(1),

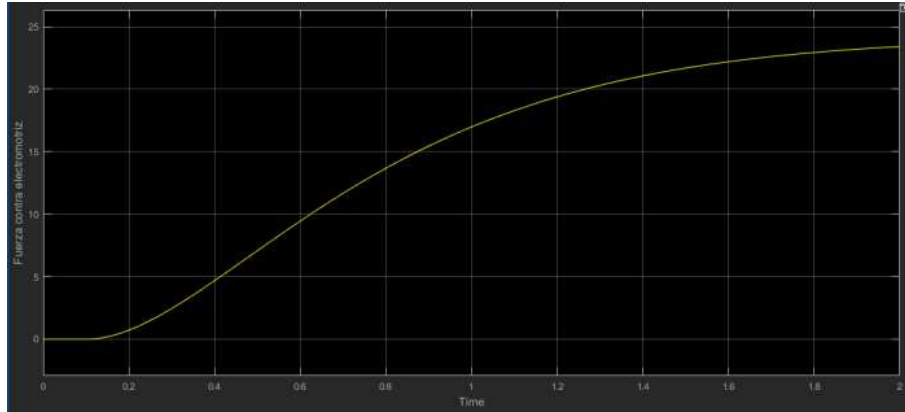


Figure 10. Counter-electromotive force as a function of time.

179-188.

Montiel, H., Martínez, F., & Jacinto, E. (2017). Visual patterns recognition in robotic platforms through the use of neural networks and image processing. *International Journal of Applied Engineering Research*, 12(18), 7770-7774.

Pongfai, J., & Assawinchaichote, W. (2017). Optimal pid parametric auto-adjustment for bldc motor

control systems based on artificial intelligence. In *International electrical engineering congress (ieecon 2017)* (p. 1-4).

Sprague, J. (2015). A sprague invention: Multiple unit train control [history]. *IEEE Power and Energy Magazine*, 13(6), 88-103.